

## Photoconductivity in sol-gel TiO<sub>2</sub> thin films with and without ammonia treatment

A. VOMVAS<sup>1\*</sup>, K. POMONI<sup>1</sup>, C. TRAPALIS<sup>2</sup>, N. TODOROVA<sup>2</sup>

<sup>1</sup>University of Patras, Physics Department, 26500 Patras, Greece

<sup>2</sup>Institute of Materials Science, NCSR "Demokritos", 15310 Ag. Paraskevi, Greece

Thin TiO<sub>2</sub> sol-gel films, with and without ammonia treatment, were prepared using the dip-coating technique and then heat treated at 500 °C. The time dependences of the photoconductivity at various light intensities were studied in vacuum and in air at 27 °C. The transient photoconductivity is very sensitive to the environment and dramatically higher than the dark one for samples both in vacuum and in air. The results are discussed in terms of the competition of the photogeneration, recombination, thermal release, and the influence of NH<sub>3</sub> treatment.

Key words: *transient photoconductivity; nanocrystalline; TiO<sub>2</sub>; ammonia treatment; sol-gel method*

### 1. Introduction

In nature, titanium dioxide occurs in three phases, such as brookite (orthorhombic), anatase (tetragonal) and rutile (tetragonal). It is amorphous for deposition temperature up to 300 °C, whereas anatase and rutile are formed typically at ~350 °C and 800 °C, respectively. Anatase nanocrystalline TiO<sub>2</sub> thin films have attracted considerable attention because of low production cost, photostability, and their application in photocatalysis, electrochromics, gas sensing, and solar cells devices.

The use of TiO<sub>2</sub> films is restricted, in a way, because of their wide band gap (3.2 eV for the anatase phase) which does not permit the response to visible light. Doping with transition metals reduces this wide band gap, but the doped materials appear to have higher concentration of recombination centres and higher instability [1]. Recently there have been reports that the introduction of small amounts of N in the TiO<sub>2</sub> lattice increases its optical absorption in the visible light, though it is not clear yet if this is an effect due to the narrowing of the optical gap [2] or to N 2p states isolated above the valence band [3, 4].

---

\*Corresponding author, e-mail: avomvas@physics.upatras.gr

In this work, we present results of measurements of transient photoconductivity,  $\sigma_p$ , for TiO<sub>2</sub> sol-gel thin films with and without ammonia treatment, heat treated at 500 °C. We study the effect of light intensity, at 27 °C, in vacuum and in air.

## 2. Experimental

TiO<sub>2</sub> thin films were prepared on carefully cleaned (in an ultrasonic water bath and then in absolute ethanol) quartz glass substrates by the dip-coating sol-gel technique. The starting solution was prepared by mixing tetrabutyl orthotitanate (Ti(C<sub>4</sub>H<sub>9</sub>O)<sub>4</sub> – TBOTi) (Aldrich) with ethyl alcohol (Panreac) in molar ratio 2:57, in a closed beaker. 10% (towards Ti) of polyethylene glycol-2000 was added to the mixture in order to obtain porous films without cracks [5]. The solution was stirred upon heating (at 70 °C) for 15 min for PEG2000 dissolution. pH of the sol was adjusted to 1.5 with the addition of 2 ml of HNO<sub>3</sub>. Distilled water (1.5 mol) was added and the solution was refluxed under dry atmosphere for 2 h at 60 °C. For completion of the hydrolysis process, the solution was kept stirred at room temperature for 20 h.

The substrate was dipped in the solution and then pulled out with a constant speed of  $3.33 \times 10^{-3}$  m/s. The gel samples were treated at 450 °C for 30 min in a Carbolite muffle furnace. The heating rate of 5 °C/min was applied. The dipping and the heating procedures were repeated in order to obtain five-layer porous TiO<sub>2</sub> films.

After that the films were heat treated at 500 °C for two hours, in either an O<sub>2</sub> atmosphere (sample A), or in an NH<sub>3</sub> atmosphere (sample B) and left to cool down slowly to 25 °C. A Thermawatt tube furnace with controlled gas flow was used. The total thickness after the final heat treatment, measured with a profilometer, was 3.22 µm for sample A and 3.10 µm for sample B.

The structure of the films was studied by the X-ray diffraction method, using a Siemens D 500 diffractometer with CuK<sub>α</sub> radiation from a secondary graphite monochromator. Photoconductivity was studied at various light intensities, as a function of time at 27 °C. All measurements were carried out in vacuum ( $10^{-2}$  Pa) and in air. The pressure in “air” was  $5.5 \times 10^4$  Pa. This pressure was chosen in order to enable measurements of the dark current and the photoconductivity with temperature (to be published). The measurements were carried out in a vacuum cryostat with coplanar electrodes separated by 0.8 mm. The temperature was controlled by an Oxford ITC4 controller and a constant bias of 5 V was applied to the sample. As a light source, a 100 W Xenon lamp was used with a full light intensity  $F_0$  of 500 W/m<sup>2</sup> on the sample, which was switched on and off every 20 min. Neutral density filters were used to vary the intensity. The current was measured with a Keithley 617 electrometer and was recorded in a computer every 10 s. The samples were annealed before any measurements at 167 °C for 90 min in order to eliminate the persisting effects of any previous light exposure.

### 3. Results and discussion

#### 3.1. Structure

The identification of the phase of the films and the grain size was done with XRD. The measurements were carried out with the following combination of slits: 1.0°/1.0° as aperture diaphragms, 0.15° as detector diaphragm and 0.15° as diffracted beam monochromator diaphragm. The measured  $2\theta$  range was scanned in steps of 0.03° in 10 s/step.

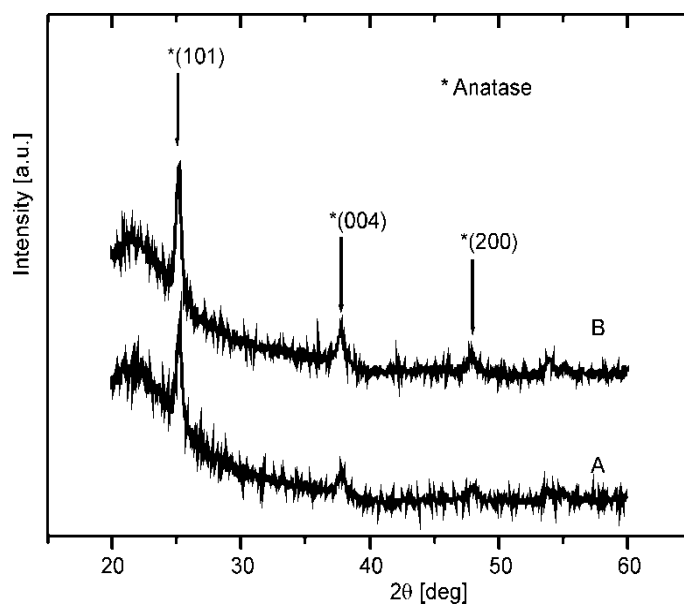


Fig. 1. XRD patterns of TiO<sub>2</sub> thin films treated in O<sub>2</sub> atmosphere (curve A) and in NH<sub>3</sub> atmosphere (curve B) at 500 °C

Figure 1 shows the XRD patterns for the undoped and N-doped samples. An intensive peak at  $2\theta = 25.30^\circ$  in both patterns corresponds to the (101) reflection while the peaks at  $38^\circ$  and  $48^\circ$  correspond to (004) and (200) reflections, respectively. These peaks confirm the presence of the anatase phase in the films with no rutile phase detected. Sherrer's semi-empirical formula  $d = K\lambda/\beta\cos\theta$  can be used for the evaluation of the average crystallite size. In the formula,  $\lambda$  is the wavelength of X-rays (0.154 nm),  $\beta$  is the full width at the half maximum (in radian),  $\theta$  is the Bragg angle, and  $K$  varies with ( $hkl$ ) and crystallite shape but is usually nearly equal to 1. From the stronger peak the mean crystallite size  $d$  was found to be 21.0 and 27.4 nm for samples A and B, respectively.

### 3.2. Photoconductivity

#### 3.2.1. Photoconductivity in vacuum

Figures 2 and 3 show the dependences of photoconductivities of samples A and B on time in vacuum at 27 °C, at various light intensities. Because of the difference in scales, the plots at 10%  $F_0$  are given as insets.

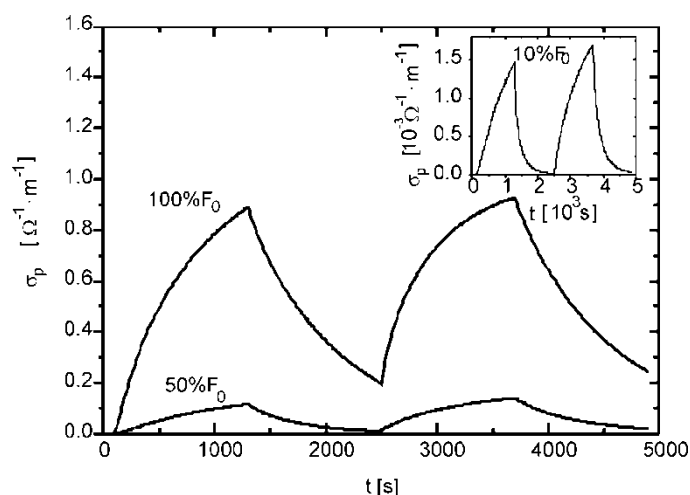


Fig. 2. The photoconductivity response of sample A in vacuum, at 27 °C, for various light intensities. The photoconductivity response, for 10% of the full light intensity ( $F_0 = 500 \text{ W/m}^2$ ), at 27 °C is given as an inset of the figure

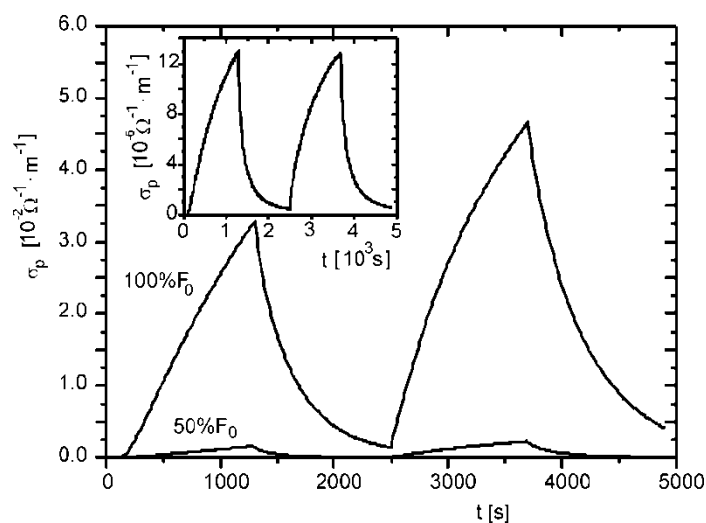


Fig. 3. The photoconductivity of sample B in vacuum, at 27 °C, illuminated at various light intensities as a function of time. The photoconductivity, for 10% of the full light intensity ( $F_0 = 500 \text{ W/m}^2$ ), at 27 °C is given as an inset of the figure

The photoconductivity of sample A (heat treated under O<sub>2</sub> atmosphere), after a quick rise, shows the usual sublinear behaviour [6, 7] resulting from the competition between photogeneration, recombination and thermal release. When the light is turned off, the decay becomes slower as time passes, due to the thermally excited electrons from the traps.

The photoconductivity  $\sigma_p$  after 20 min of illumination with 100%  $F_0$  is  $0.89 \Omega^{-1}\cdot\text{m}^{-1}$  for sample A. This value is found to be nine orders of magnitude higher than its dark conductivity  $\sigma_d$ . This behaviour can be attributed to a high porosity and high density of trapping states in the energy gap of the sample. At the end of the second illumination, the  $\sigma_p$  maximum value shows an increase of about 4% compared to that at the end of the first illumination. Some traps, which remained still filled at the end of the decay period, allow the excitation of more photogenerated electrons to the conduction band, thus increasing  $\sigma_p$  [8]. The observed increase is not high, since the recombination rate at this level of illumination is significant. At 50%  $F_0$ , where the recombination rate is lower, the corresponding increase is higher (19%), as expected. At 10%  $F_0$ , the increase at the end of the second illumination is somehow lower (16%) than that at 50%  $F_0$  because of the lower density of traps that still remained filled at the end of the decay time at this low level of intensity.

In the case of sample B, heat treated under NH<sub>3</sub> atmosphere (Fig. 3),  $\sigma_p$  shows a less pronounced sublinear behaviour, indicating that the thermal release rate dominates after the initial stage of illumination.  $\sigma_p$  at the end of the 20 min of illumination with  $F_0$  was  $3.3 \times 10^{-2} \Omega^{-1}\cdot\text{m}^{-1}$ , which is more than eight orders of magnitude higher than its  $\sigma_d$  but smaller than the photoconductivity of sample A. This was caused by the ammonia treatment, which created additional oxygen vacancies which increased the dark conductivity, but acted as recombination centres [9] upon illumination and did not permit the further increase of  $\sigma_p$ .

The increase in the photoconductivity values at the end of the second illumination period was high enough (about 43%) for the 100% and the 50%  $F_0$ , compared to that of the first illumination. This is caused by the fact that the concentration of the trapping states that remained filled was high enough because of the modification that the ammonia treatment caused. As for the 10%  $F_0$ ,  $\sigma_p$  at the end of the second illumination was found to have the same value as in the first illumination, because of the decrease of density of the filled traps at the end of the preceded decay time.

### 3.2.2. Photoconductivity in air

The photoconductivity responses of samples A and B, at 27 °C, in air, at various light intensities, are shown in Figs. 4 and 5, respectively. Because of the difference in scales, the plots at 10%  $F_0$  are given as insets.

At the beginning of illumination in air with  $F_0$ ,  $\sigma_p$  of both samples increases rapidly reaching a maximum and then slowly decreases. This behaviour suggests that recombination is the predominant mechanism in air. The  $\sigma_p$  values are again much higher than the respective  $\sigma_d$  ones but lower than their photoconductivities in vacuum.

This different behaviour in vacuum and in air indicates that when the pressure increases the then created electron scavengers  $O_2^-$  result in the decrease of  $\sigma_p$  [10]. When the light is switched off,  $\sigma_p$  falls rapidly in both samples indicating again the significant role of recombination in air.

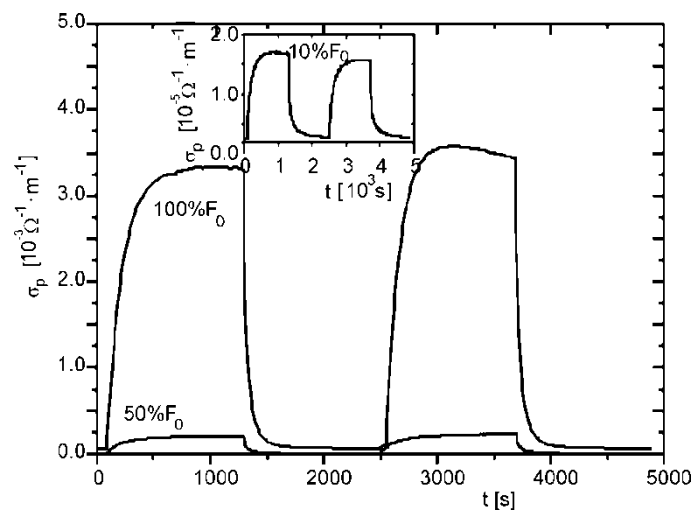


Fig. 4. The photoconductivity response of the sample A in air, at 27 °C, for various light intensities. The photoconductivity response, for 10% of the full light intensity ( $F_0 = 500 \text{ W/m}^2$ ), at 27 °C is given as an inset of the figure

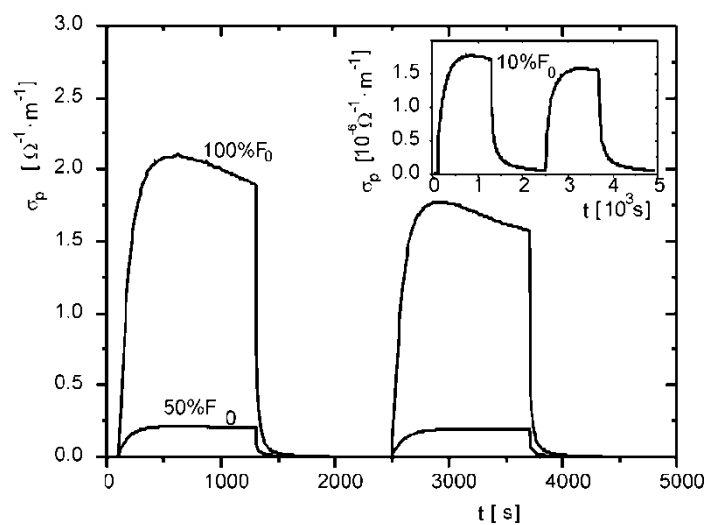


Fig. 5. The photoconductivity of sample B in air, at 27 °C, illuminated at various light intensities as a function of time. The photoconductivity for 10% of the full light intensity ( $F_0 = 500 \text{ W/m}^2$ ), at 27 °C is given as an inset of the figure

In the case of sample A, at full light intensity  $F_0$ , photoconductivity reaches quickly high values ( $3.2 \times 10^{-3} \Omega^{-1} \cdot \text{m}^{-1}$  at the end of the first illumination). When the light is switched off,  $\sigma_p$  decays rapidly almost near to the initial dark value. During the second illumination, photoconductivity reaches quickly its maximum, then falls slowly and at the end of this illumination period its value is about 3% higher than that at the end of the first illumination. It seems that even in air some traps remain occupied at the end of the decay time and permit the photogenerated electrons to move quickly to the conduction band and increase the photoconductivity. The observed slow fall may be attributed to the recombination rate that is dominant from the very early stage of illumination.

As the light intensity decreases, the photoconductivity of sample A takes, as is expected, lower values. For 50%  $F_0$ ,  $\sigma_p$  at the end of the second illumination period shows a higher increase (about 11%) compared to that of the first one, as a consequence of the lower recombination rate at this level of illumination, while for 10%  $F_0$ , a decrease in  $\sigma_p$  of almost 6.5% is observed. It seems that the thermal release rate becomes significant because of the low photogeneration rate during the second illumination period. This enhances the recombination rate and causes a decrease in photoconductivity.

When sample B is illuminated in air at various light intensities, the corresponding photoconductivity (Fig. 5) follows a similar behaviour to that of sample A but with  $\sigma_p$  values lower ( $1.9 \times 10^{-4} \Omega^{-1} \cdot \text{m}^{-1}$  at the end of the first illumination), as the modification caused by the NH<sub>3</sub> treatment, adds recombination centres in the gap of the TiO<sub>2</sub> semiconductor.

For all used light intensities, a decrease in photoconductivity values at the end of the second illumination is observed and can be attributed to a high recombination rate created by the ammonia treatment.

#### 4. Conclusions

A study of the transient photoconductivity of thin TiO<sub>2</sub> sol-gel films, with and without ammonia treatment, in vacuum and in air, as a function of the illumination time and the light intensity, has been presented in this work.

The photoconductivity for full light intensity  $F_0$  is much higher than the dark conductivity of both samples, in vacuum and in air.

In vacuum, the value of  $\sigma_p$  for samples A and B at the end of the second period of illumination was found to be higher than in the first one for almost all the used light intensities, as a result of the competition between recombination and the release of electrons from traps.

In air, at the end of the second illumination, the values of  $\sigma_p$  were found to be higher than in the first one for sample A for light intensities 100% and 50%  $F_0$ . On the

contrary, for sample B in air,  $\sigma_p$  was lower at the end of the second illumination period for all light intensities because of the  $\text{NH}_3$  treatment.

#### Acknowledgements

The authors would like to thank John Hiotelis for the evaporation of electrodes on the samples.

#### References

- [1] SAKATA Y., YAMAMOTO T., OKAZAKI T., IMAMURA H., TSUCHIYA S., Chem. Lett., 12 (1998), 1253.
- [2] ASAHI R., MORIKAWA T., OHWAKI T., AOKI K., TAGA Y., Science, 293 (2001), 269.
- [3] IRIE H., WATANABE W., HASHIMOTO K., J. Phys. Chem. B, 107 (2003), 5483.
- [4] LINDGREN T., MWABORA J.M., AVENDANO E., JONSSON J., HOEL A., GRANQVIST C., LINDQUIST S., J. Phys. Chem. B, 107 (2003), 5709.
- [5] GUO B., LIU Z., HONG L., JIANG H., LEE J., Thin Solid Films, 479 (2005), 310.
- [6] SCHWARZBURG K., WILLING F., Appl. Phys. Lett., 58 (1991), 2520.
- [7] POMONI K., VOMVAS A., TRAPALIS C., Thin Solid Films, 479 (2005), 160.
- [8] EPPLER A.M., BALLARD I.M., NELSON J., Physica, E, 14 (2002), 197.
- [9] LINDGREN T., LU J., HOEL A., GRANQVIST C., TORRES G., LINDQUIST S., Sol. Energy Mater. Sol. Cells, 84 (2004), 145.
- [10] WEIDMANN J., DITTRICH T., KONSTANTINOVA E., LAUERMANN I., UHLENDORF I., KOCH F., Sol. Energy Mater. Sol. Cells, 56 (1999), 153.

*Received 22 June 2006*

*Revised 20 March 2007*